Motive performance of a new type of vertical axis rotor estimated by CFD analysis

Yuki Takahashi[*], Yasuzumi Fujimori[**], Hiroki Yasuma[**],
Hajime Yasui[**] and Nobuo Kimura[**]

[*] Graduate School of Fisheries Sciences, Hokkaido University, Japan
[**] Faculty of Fisheries Sciences, Hokkaido University, Japan

Abstract

Until now, the water lifting system using wind power was developed to reduce the energy consumption in the bio-farming. In this study, a new type of vertical axis rotor used in the bio-farming was planned and its motive performance was investigated by CFD analysis. The rotor unit is composed of the outer and inner rotors, the gyromill rotor with three wings in outside and the savonius rotor in inside.On the condition of the parameters, angle of attack of gyromill wing θ was set as 0 to 30°, and angle of flow direction ϕ was 0, 30, 60, and 90°. When the condition of ϕ=0°, large torque value was observed. In contrast, when ϕ=30°, torque value was decreased according to the increase of θ. The current was interrupted by the gyromill wing (ϕ=0°) or savonius rotor (ϕ=30°), and these are important for characteristics of motive performance.

Keywords: CFD analysis, Savonius rotor, Gyromill rotor

1. Introduction

This study was conducted as a part of the project to develop a bio-farming system using renewable energy which is implemented by Hakodate Marine Bio Cluster supported by the Ministry of Education, Japan. Until now, the water lifting system using wind power by the savonius rotor was developed to reduce the energy consumption in the bio-farming [1], [2].

The savonius rotor has an advantage to be rotated at the low wind velocity, which produce the high torque even at low wind velocity [3]. In addition, the savonius rotor

could be made and maintained cheaply. This type of rotor, therefore, is used widely in small-scale plants that need a wind power. However, it is known that the savonius rotor is inefficient in high wind velocity, because this rotor is rotated by the drag produced by wind [4]. By contrast, the gyromill type rotor, which is vertical axis type similar to savonius rotor, is efficient in high wind velocity because of rotation by the lift-force. Although, it required large torque when starting the rotation [5].

This study proposes a new type vertical axis rotor, composite design of the savonius and gyromill rotor, and investigates the motive performance of new rotor using CFD (Computational Fluid Dynamics) analysis. Moreover, we discuss based on the calculated results what is important factor to obtain the optimal design.

2. Method

2.1 New type vertical axis rotor

Dimensions of proposed new rotor are shown in Fig.1. The rotor is composed of the outer and inner rotor, the gyromill rotor with three wings in outside and the savonius rotor in inside. The span of outer wing is 1.6 m, the maximum wing thickness is 0.047m and the diameter is 1.2 m. The height of savonius rotor is 1.0 m, and the diameter is 0.5 m. This rotor makes a counterclockwise turn.

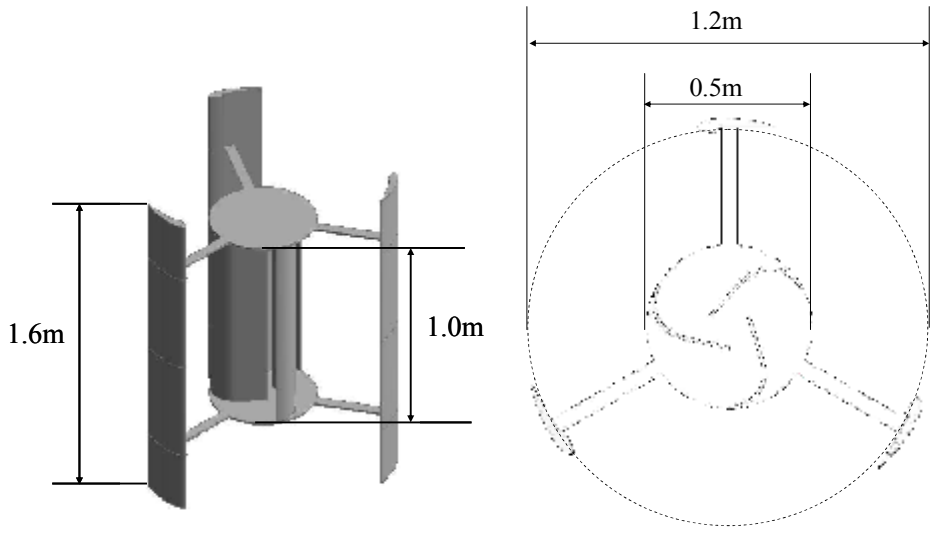

Fig.1 Dimensions of new type of vertical axis rotor

2.2 Method of analysis

The fluid analysis software ANSYS CFX (CYBERNET Inc.) is used for the calculation of torque value, and visualization of pressure distribution and streamline. Here, the torque of counterclockwise direction is defined plus. This software solves Navier-Stokes equation using finite volume method (FVM). In the calculation, tetrahedral mesh is used. Number of the elements is about 500000. Computational area is the cube of 10.0m on a side, and the rotor model is positioned at the center of the cube (Fig.2). The current velocities at the inlet are set as the verticallly uniform horizontal flow with 7.0 m/s. The value of the relative pressure at the outlet and the opening are set as 0.0 Pa. The current velocities at the rotor surface are 0.0 m/s in the condition of no slip (Table.1). The SST (Shear Stress Transport) model is employed as the turbulent flow model and kind of fluid is set as air. On the computational condition, the air density is 1.185 kgm^{-3}, the temperature is 25℃, and the kinematic viscosity is 1.831×10^{-5} m^2s^{-1}.

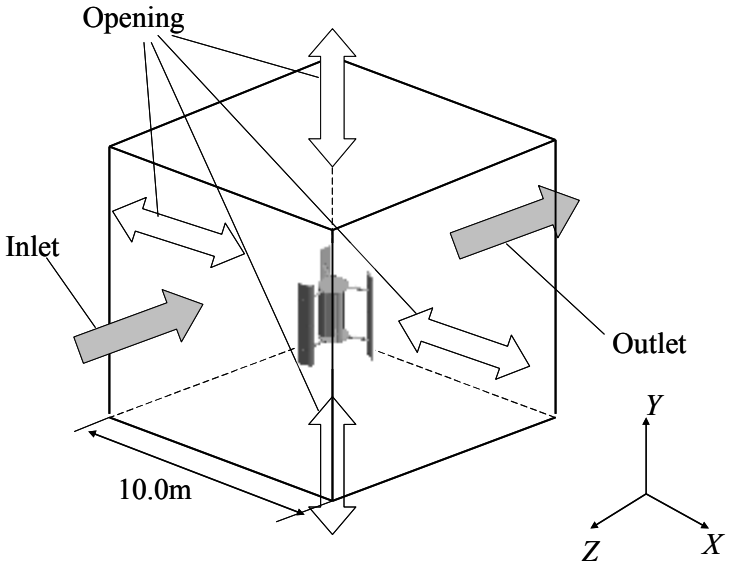

Fig.2 Computational area

Table.1 Detail of boundary condition

position in Fig.2	boundary type	option	value
Inlet	inlet	Normal Speed	7.0m/s
Outlet	outlet	Average Static Pressure	relative pressure 0.0Pa
Opening	opening	Opening Pressure and Direction	relative pressure 0.0Pa
surface on the rotor	wall	No Slip	

Fundamental equation Considering the law of conservation of mass, and supposed an incompressible flow of a Newtonian fluid, density ρ is constant. Then, the continuity equation is derived as follows:

$$\frac{\partial u}{\partial x}+\frac{\partial v}{\partial y}+\frac{\partial w}{\partial z}=0 \tag{1}$$

Here, u, v, w are flow velocities in x, y, z coordinates. Following equations are derived from law of the conservation of momentum.

$$\begin{aligned}
\frac{Du}{Dt}&=\frac{\partial u}{\partial t}+u\frac{\partial u}{\partial x}+v\frac{\partial u}{\partial y}+w\frac{\partial u}{\partial z}=-\frac{1}{\rho}\frac{\partial u}{\partial x}+\upsilon\nabla^2 u+F_x\\
\frac{Dv}{Dt}&=\frac{\partial v}{\partial t}+u\frac{\partial v}{\partial x}+v\frac{\partial v}{\partial y}+w\frac{\partial v}{\partial z}=-\frac{1}{\rho}\frac{\partial v}{\partial y}+\upsilon\nabla^2 v+F_y\\
\frac{Dw}{Dt}&=\frac{\partial w}{\partial t}+u\frac{\partial w}{\partial x}+v\frac{\partial w}{\partial y}+w\frac{\partial w}{\partial z}=-\frac{1}{\rho}\frac{\partial w}{\partial z}+\upsilon\nabla^2 w+F_z
\end{aligned} \tag{2}$$

Here, ρ is density and pressure, μ is static coefficient of viscosity, and υ is kinematic viscosity. This equation is called as Navier-Stokes equation.

Each term of middle part of equation (2) is called as momentum term, advective term, and each term of right part is called as pressure term, viscous term, and external force term, respectively.

Here,

$$\upsilon=\frac{\mu}{\rho} \tag{3}$$

$$\nabla^2=\frac{\partial^2}{\partial x^2}+\frac{\partial^2}{\partial y^2}+\frac{\partial^2}{\partial z^2} \tag{4}$$

2.3 Parameter

Here, θ, angle of attack of gyromill wing, and ϕ, angle of flow direction were defined as parameters (Fig.3). In this study, θ was set as 0, 5, 10, 20 and 30°, and ϕ was 0, 30, 60 and 90°.

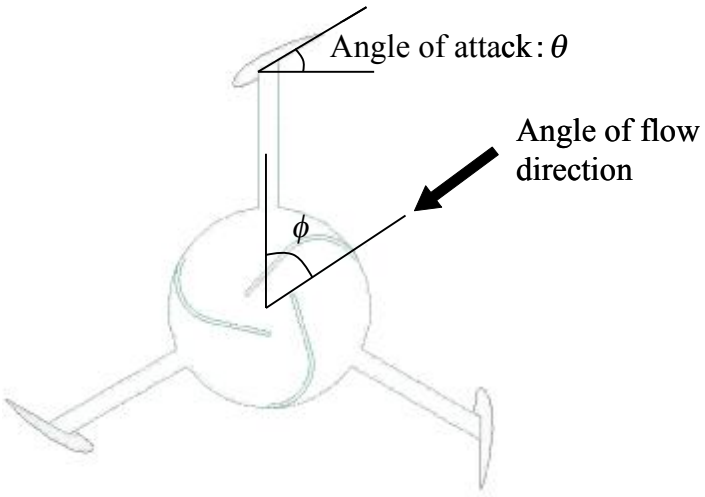

Fig.3 Parameters of analysis

3. Result

The relationship between the estimated torque value and the angle of flow direction (ϕ) was shown in Fig.4. Large torque value was obtained in condition of ϕ=0°. While torque value became small when ϕ=30°. The negative value was estimated when θ=20, 30°.

Next, the pressure distribution and streamline around the rotor were visualized in the model of θ=0°, ϕ=0° (the torque value is 2.04 Nm), θ=20°, ϕ=0° (the torque value is 5.38 Nm), θ=0°, ϕ=30° (the torque value is 1.63 Nm), and θ=20°, ϕ=30° (the torque value is -0.31 Nm).

First, the models of θ=0° and θ=20° were compared when the condition of ϕ=0°. The pressure distributions in the model of θ=0°, ϕ=0° and θ=20°, ϕ=0° were shown in Fig.5 (a), (b), and the streamline around the rotor were shown in Fig.6 (a), (b). In the wing of the lower right in Fig.5 (a), (b), the pressure of the outer side when θ=20° was smaller than that when θ=0°. And in the wing of lower left in Fig.5 (b), the high pressure was observed in the inner side. On the other hand, the little difference in pressure was observed in the savonius rotor. In the wing of the right in Fig.6 (a), the flow separation was observed. However, in the model of θ=20° shown in Fig.6 (b), the flow separation was not found. Therefore, the torque value when θ=20° was lager than θ=0°.

Second, the models of θ=0° and θ=20° were compared when the condition of ϕ=30°. Pressure distributions in the model of θ=0°, ϕ=30° and θ=20°, ϕ=30° were shown in Fig.7 (a), (b), and streamlines around the rotor were shown in Fig.8 (a), (b). In the right-sided gyromill wing of Fig.7 (a), the pressure of the inner side was higher than that of the outer side. However, in Fig.7 (b), the pressure of the outer side was higher than

that of the inner side. In Fig.8 (a), (b), when θ=20°, the flow separation was observed in the right-sided gyromill wing. However, when θ=0°, the flow separation was not found. In addition, the large difference in pressure was observed in the savonius rotor, and the difference of pressure around the outer wing in backward stream became small. Moreover, the low velocity current was observed around the outer wing.

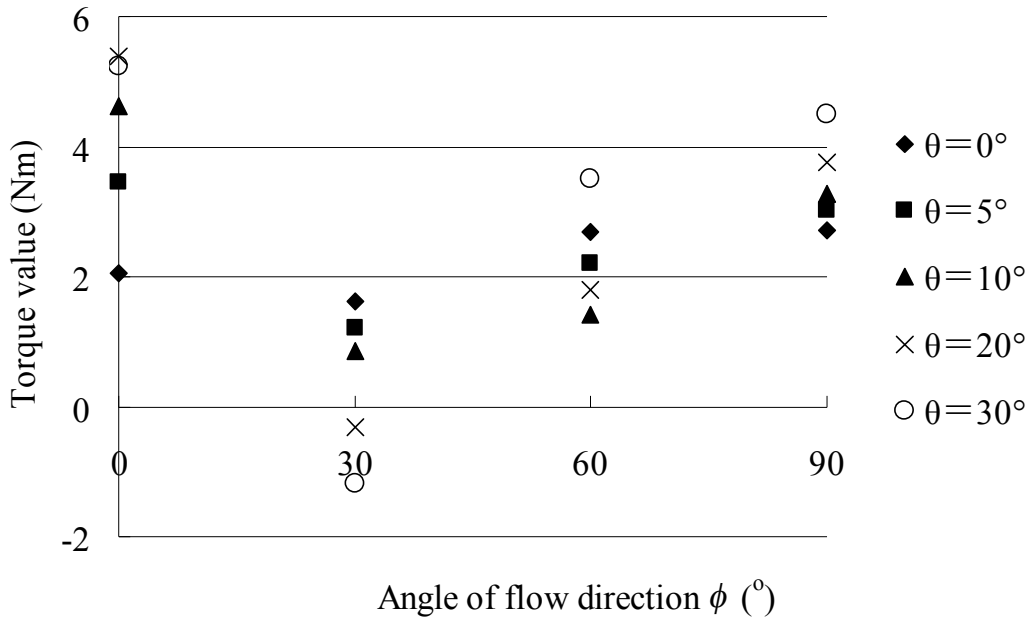

Fig.4 Relationship between the estimated torque value and ϕ

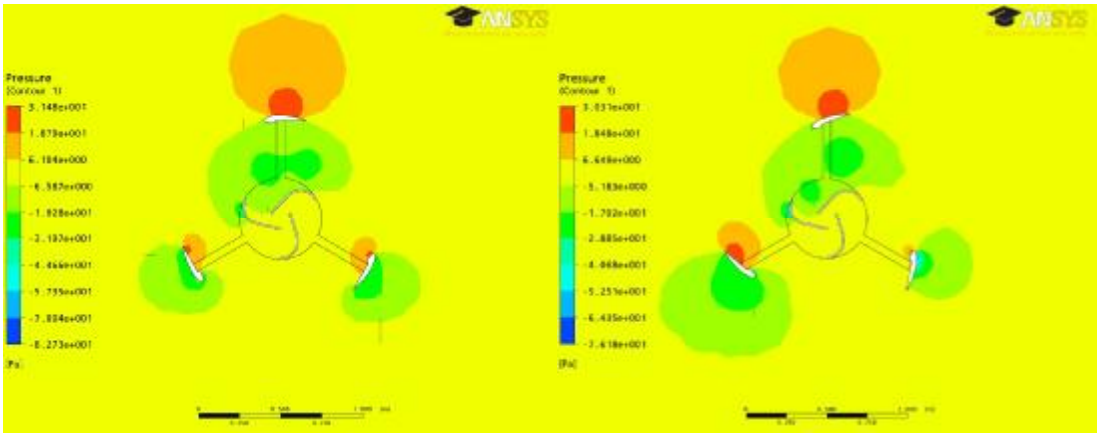

(a) (b)

Fig.5 Pressure distribution (a: θ=0°, ϕ=0°, b: θ=20°, ϕ=0°)

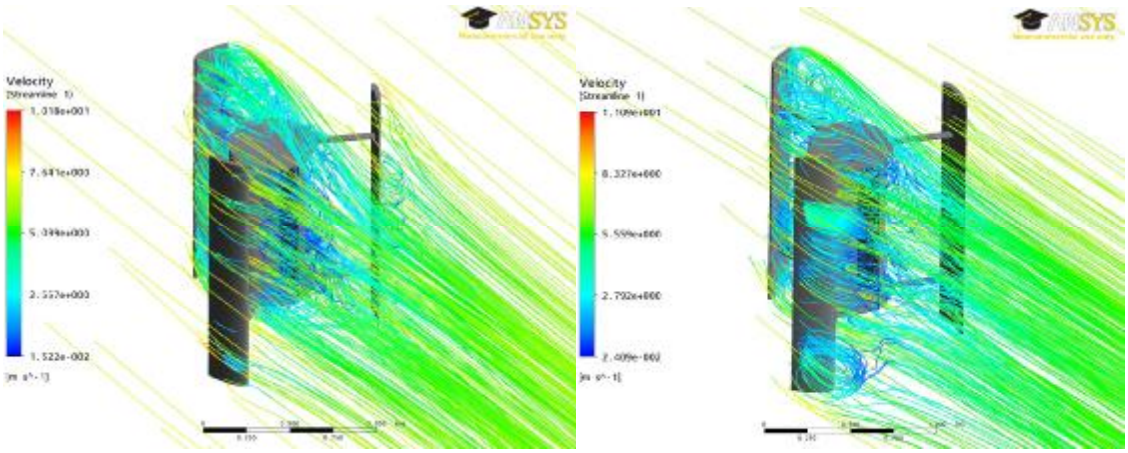

(a) (b)

Fig.6 Stream line around the rotor (a: θ =0°, ϕ =0°, b: θ =20°, ϕ =0°)

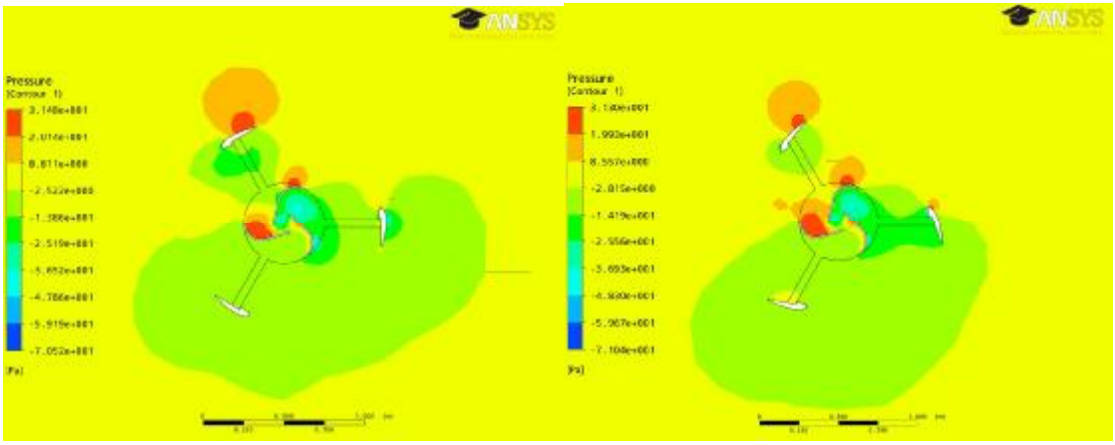

(a) (b)

Fig.7 Pressure distribution (a: θ =0°, ϕ =30°, b: θ =20°, ϕ =30°)

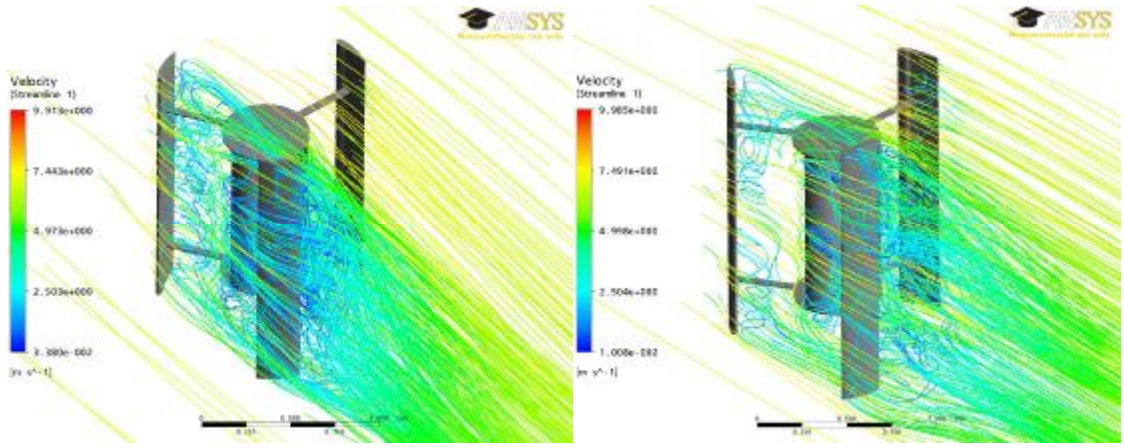

(a) (b)

Fig.8 Stream line around the rotor (a: θ =0°, ϕ =30°, b: θ =20°, ϕ =30°)

4. Conclusion

When ϕ=0°, the current was interrupted by the outer wing and the current velocity of around savonius rotor became small. Then, the slight difference of pressure was observed around there (Fig.5 (a)). On the other hand, the current velocities around the all outer wings became fast, and the large difference in pressure distribution was observed around these wings. This implies that the effect of outer wing was larger than the savonius rotor in this flow direction

When ϕ=30°, the current was not interrupted by the outer wing and high velocity current was observed around the savonius rotor. Therefore, the effect of savonius rotor was seemed to be larger than that when ϕ=0°. However, the backward stream was interrupted by the savonius rotor, then, the difference in pressure of around the outer wing became small (Fig.7 (a), (b)). It is known that gyromill rotors are rotated by the lift force, and also the drag force in the backward wing [5]. However, in this direction, the outer wing in the backward stream cannot obtain drag force. Additionally, the right-sided wing blocked rotation. Therefore, the torque value was decreased according to the increase of θ (Fig.4).

The current was interrupted by the gyromill (case ϕ=0°) or savonius rotor (case ϕ=30°), and it was important for characteristics of motive performance in the steady condition. In this analysis, when θ=0, 5 and 10°, the torque value became positive value in all directions. Therefore, it was considered that θ should be set between 0 and 10° in the motive performance.

5. Acknowledgement

This research has been financially supported by the knowledge cluster initiative of the Ministry of Education, Cluster, Sports, Science and Technology from 2009. And I wish to thank assistant professor Kazuyoshi Maekawa for the advice.

References

[1] Junya Yamashita, Yasuzumi Fujimori, Yuki Takahashi, Hajime Yasui, and Nobuo Kimura: Development of a wind pump system with Savonius Rotor using Computing Aided Engineering technique, Mathematical and Physical Fisheries Science, Vol.8, 42-53pp, 2010

[2] Masaaki SATOH: Research on fluid characteristics of savonius rotor, Hokkaido University, Graduation thesis, 2011

[3] Takenori OGAWA: Research on savonius rotor, Japan society of Mechanical Engineers, Vol.49, 441, 976-984pp, 1983

[4] N. Fujisawa, F. Gotoh: Visualization study of the flow in and around a Savonius rotor, Experiments in Fluid 12, 407-412pp, 1992

[5] Fumio MATSUKI: Development of gyromill type rotor, Journal of JWEA, Vol.31, No.2, 144-147pp, 2007

[6] Kensaku NONOURA, Shigeaki KURODA, Binghu PIAO, Makoto TSUBOKURA: Flow Analysis around Gyro-Mill Type Wind turbine, Japan society of Mechanical Engineers, No.05-1, 163-164pp, 2005-9.19～22

Academic backgrounds:

Yuki Takahashi

04/2006 – 03/2010	Faculty of Fisheries Hokkaido University, Japan
04/2010 –	Master's course of Graduate School of Fisheries Hokkaido University, Japan
Research field:	Fisheries Engineering, Computational Fluid Dynamics

Yasuzumi Fujimori

04/1994 – 03/2005	Assistant Professor, Hokkaido University, Japan
04/2005 – 04/2010	Associate Professor, Hokkaido University, Japan
05/2010 –	Professor, Hokkaido University, Japan

Research field: Fishery process and the selectivity of fishing implements

Hiroki Yasuma

04/2004 – 03/2010 Postdoctoral Fellow, Field Science Center for the Northern Biosphere, Hokkaido University, Hokkaido, Japan

04/2010 – 03/2011 Researcher, Fisheries Technology Department, Kyoto Prefectural Agriculture, Forestry and Fisheries Technology Center, Kyoto, Japan

04/2011 – Associate Professor, Hokkaido University, Japan

Research field: Fishery acoustics, Mesopelagic community

Hajime Yasui

04/1987 – 03/1994 Assistant Professor, Hokkaido University, Japan

04/1994 – 03/2010 Associate Professor, Hokkaido University, Japan

04/2010 – Professor, Hokkaido University, Japan

Research field: Increase biology of the marine large scale alga

Nobuo Kimura

04/1986 – 03/1991 Assistant Professor, Hokkaido University, Japan

04/1991 – 03/2005 Associate Professor, Hokkaido University, Japan

04/2005 – Professor, Hokkaido University, Japan

Research field: Seakeeping quality of fishing vessel, Fishing Engineering, Fluid dynamics